Nonlinear Finite Element Analysis of Bone-Implant Contact in Three Short Dental Implant Models with Varying Osseointegration Percentages

Dawit Bogale Alemayehu * , Masahiro Todoh , Song-Jeng Huang

Posted Date: 29 August 2024

doi: 10.20944/preprints202408.2180.v1

Keywords: Biomechanical; Osseo-integration; Low-density; High-density; Cancellous bone; Short dental implant; Finite element analysis; bone-implant contact

Article

Nonlinear Finite Element Analysis of Bone-Implant Contact in Three Short Dental Implant Models with Varying Osseointegration Percentages

Dawit Bogale Alemayehu [1,*], Masahiro Todoh [2] and Song-Jeng Huang [3]

[1] Division of Human Mechanical Systems and Design, Graduate School of Engineering, Hokkaido University, Sapporo 060-8628, Japan
[2] Division of Mechanical and Aerospace Engineering, Faculty of Engineering, Hokkaido University, Sapporo 060-8628, Japan
[3] Department of Mechanical Engineering, National Taiwan University of Science and Technology, Taipei 10607, Taiwan
* Correspondence: zetseatdawit2018@gmail.com

Abstract: Background/Objectives: Dental implants have become a cornerstone of restorative dentistry, providing a long-lasting method for tooth replacement. The degree of osseointegration has a significant effect on biomechanical stability at the bone-implant contact (BIC), determining the continued efficacy of these implants. However, the exact consequences of changing osseointegration levels on different implant designs, especially in bones with variable densities, are not well known. ; **Methods**: This study used 3D finite element analysis (FEA) to look at the biomechanical performance of three short dental implants: BioMet 3iT3, Straumann® Standard Plus Short -Regular neck (SPS-RN), and Straumann® Standard Plus Short-Wide neck (SPS-WN). This paper tests the implants at four stages of osseointegration: 25%, 50%, 75%, and 100% in both high-density (Bone Type III) and low-density (Bone Type IV) cancellous bone. It also created and examined realistic CAD models under static occlusal loading conditions to assess stress distribution and major strains at the bone-implant contact.; **Results**: The study discovered that as osseointegration increases, von Mises stress and principal strains go down significantly for all implant types. The SPS-WN implant had the lowest strain values, especially for bone with low density. These reductions demonstrate increased mechanical stability as the bone-implant interface becomes more capable of dispersing mechanical stresses, minimizing the potential for localized deformation and bone resorption.; **Conclusions**: The results highlight the importance of achieving optimum osseointegration to reduce mechanical stress and increase the lifespan of dental implants. The SPS-WN type implant performed better in biomechanical tests than the others, especially when bone conditions were not ideal. This makes it a great choice for clinical applications that need long-term implant success.

Keywords: biomechanical; Osseo-integration; low-density; high-density; cancellous bone; short dental implant; finite element analysis; bone-implant contact

1. Introduction

Dental implants have transformed the sector by offering a long-lasting, functionally efficient, and aesthetically beautiful alternative to missing teeth [1,2]. Dental implants aim to integrate directly with the jawbone, a process known as osseointegration, unlike typical dental prostheses like dentures or bridges[3–5]. This integration is critical to the implant's long-term durability and success because it enables it to operate like a natural tooth root, firmly supporting the overlying prosthesis[6–8]. Short dental implants have become a more prevalent dental restorative treatment, mainly for individuals with poor bone health[9–11]. These implants are a stable and durable strategy for restoring lost teeth, with significant benefits over conventional dentures or bridges. Unlike standard dental artificial

 doi:10.20944/preprints202408.2180.v1

teeth, short dental implants directly connect into the jawbone through a process known as osseointegration[12,13]. This bonding is important for recovering teeth's function in addition to their original physique because it enables the implant to act analogously to an actual tooth root, firmly holding the prosthesis.

However, the recipient's bone qualities, along with the surgical approach and implant quality, heavily influence the success of dental implants[14–16]. In recipients with an appropriate quantity of bone and density, osseointegration typically occurs readily, resulting in an anchored and safe implant. However, a considerable minority of patients, notably those with low bone density or height, have major difficulties in attaining effective osseointegration[12,17–19]. The efficacy of dental implants is intimately related to osseointegration, in which bone forms around and binds with the implant surface, forming a firm base[20–22]. These properties are particularly prevalent in Bone Types III and IV, where the bone is either less thick or exceedingly porous, thereby increasing the likelihood of malfunctioning implants[23–26].

Short dental implants have emerged as a potential solution for individuals with poor bone health in the context of dental implantology[27–29]. Traditionally, invasive operations like bone grafting or sinus lifts treated patients with insufficient bone height or density, augmenting the bone and providing a solid foundation for standard-length implants[30]. While successful, these techniques are linked to greater surgical complexity, longer recovery periods, and higher expenses[31–33]. Short implants, typically less than 7 mm in length, produce adequate results in situations where regular implants may be prohibited[34–37]. Short dental implants have grown in popularity because of their potential to offer excellent results in situations when regular implants would be undesirable. Small implants, when implanted in the accessible bone, may eliminate the need for extensive grafting operations in patients with limited bone height, particularly in the posterior maxilla[38–40]. Also, when a patient has low bone density, short implants put less stress on the bone around them. This may help the distribution of occlusal force and lower the risk of overworking the bone-implant contact[34,41,42].

The practical use of short dental implants has benefited from advancements in implant design and surface technology, as they have proven to enhance osseointegration, even in challenging bone conditions[13,43,44]. Despite these advances, research into the biomechanical behavior of short implants with varied degrees of osseointegration is still underway. Understanding how varied degrees of osseointegration influence stress distribution and strain at the bone-implant interface is critical for optimizing implant designs and improving patient outcomes, especially in individuals with low bone density [45–47].

A variety of industries, including automobile engineering[48,49] , dentistry [50,51], and heat transfer studies [52], use the Finite Element Method (FEM), an advanced and adaptable computational method. In the field of dental implantology, FEM is critical for biomechanical characterization of dental implants and surrounding bone structures[50,51]. This technology enables researchers and physicians to anticipate how implants will interact with bone in various settings by simulating and evaluating complex mechanical characteristics in detail [53]. Researchers have widely used FEM to estimate stress distribution inside dental implants, as well as in compact and spongy bone, under various loading conditions and degrees of osseointegration [24].

This research study significant biomechanical effects of different osseointegration percentages in three different short dental implant models: BioMet 3iT3, SPS-RN, and SPS-WN. The main goal is to find the best short dental implant among these options for replacing natural teeth in people with low bone density and not enough bone height, specifically less than 7 mm. Traditional approaches to treating these difficult illnesses sometimes include intrusive operations such as bone grafting, which are associated with greater risks, longer recovery periods, and higher costs. Short dental implants, on the other hand, are a less intrusive option that may eliminate the need for bone augmentation while still giving effective and long-lasting results. To do this, we used nonlinear three-dimensional finite element analysis (FEA) to model how the bone and implant interact when the bone density and osseointegration are different. The study looked at a lot of important things, like the highest stress at the bone-implant contact (BIC), especially at the implant neck and bone hole locations, as well as the

 doi:10.20944/preprints202408.2180.v1

highest and lowest primary strains at the BIC. Furthermore, we investigated the distribution of maximal von Mises stresses across each of the three short dental implants. These biomechanical factors are critical for determining the implants' capacity to efficiently distribute mechanical loads, reduce localized stress concentrations, and improve overall stability and durability. This study aims to shed light on the comparative performance of these short implants in clinical settings where bone grafting is not feasible. The goal of this research is to help doctors choose the optimal implant for patients with low bone density and restricted bone height by determining the implant type that provides the highest biomechanical performance under compromised bone circumstances. Finally, this study not only adds to the current body of evidence, but it also has the potential to impact medical decisions, resulting in better patient outcomes and defining a new standard for dental implantology in difficult situations.

2. Materials and Methods

2.1. CAD Geometry Design

In terms of size and shape, three dimensional geometric models of the premolar implant and the peri - implant bone were considered to be closely realistic [54]. based on previous work both compact and spongy bone regions were improved since the implant depth touch both. Model I was the Biomet 3iT3 Short implant with dimension of 5mm(D) x 6mm(L), which was obtained from (Zimmer Biomet Dental, USA), Model II was the Standard Regular neck SRN- Straumann® Standard Plus Short (SPS) Implants, at 4 mm long, 4.1 mm diameter, Straumann, this implant design was gotten from (Holding AG, Peter Merian-Weg 12, 4002 Basel, Switzerland), and Model III was the Standard Wide

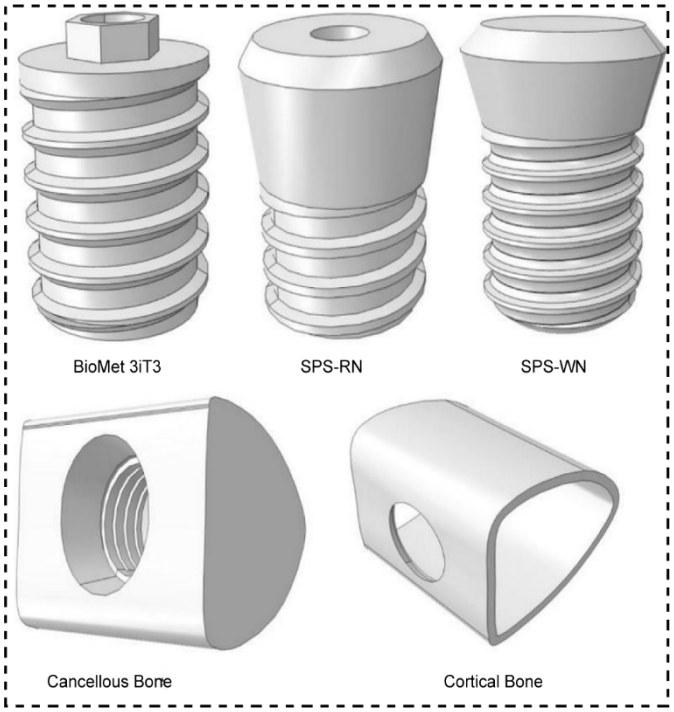

Figure 1. 3D CAD model of three dental implant and bone.

Neck SWN- Straumann Standard Plus Short (SPS) Implants, at 4 mm long, 4.8 mm diameter, Straumann, and this implant design was obtained from (Holding AG, Peter Merian-Weg 12, 4002 Basel, Switzerland), and bone were designed using CATIA V5-6R2017 software (Dassault Systèmes, aircraft manufacturer AVIONS MARCEL DASSAULT, French). A bone block model was also built based on a cross - sectional image of the molar region's human mandible, 15 mm high, 12 mm wide and 12 mm thick, and the trabecular bone in the center was surrounded by 1 mm of cortical bone. The implant was placed in the bone block that was cortical and cancellous.

 doi:10.20944/preprints202408.2180.v1

2.2. Three-Dimensional Finite Element Analysis (FEA)

After modeling the solids, geometries were exported to FEA software for pre- and post-processing (ABAQUS 2017, Dassault Systèmes SIMULIA, Johnston, Rhode Island, USA), to obtain meshes of specially for our case, geometries are very complicated, in such situation it is used tetrahedral elements specifically quadratic tetrahedral element with 10 node (C3D10) for each model (Table 3). The mechanical properties of each simulated material were attributed to the meshes by using previously published values in the literature (Table 3) [55–57]**.** The bone materials were anisotropic and implant material is to be homogeneous, isotropic and linearly elastic [58].

All contacts between implant/bone and bone/bone were simulated with no slipping between the surfaces its is would be with surface to surface and selected "finite sliding". It is also defined the interaction property as well. For this contact is given "tangential behavior" and friction and selected "rough". This in turn will prevent any slip between the surfaces. Most importantly all contacts were simulated by symmetric contacts. Constraint definitions were established as fixed in the axes (x, y and z) at the mesial and distal surfaces of the cortical and trabecular bone. All other model surfaces were unrestricted. For the static occlusal load, concentrated Oblique force was 380 N at a specific four points on the internal slope of the cusps which is equivalent to a pressure of 100MPa[59,60].

2.3. Material Properties

A set of fabric elastic properties are allotted to the jaw bone models. Ideally, the properties ought to represent the property of bone. Bone is taken into account anisotropic as a result of it shows different mechanical properties once measured in several directions (in the identical sample) [61]. Bone can be assumed transversely isotropic based on the elastic moduli of cortical bone buccolingual and infero-superior directions [55,57] and that of cancellous bone in the direction of buccolingual and mesiodistal [55,62] are not significantly different. Hence bone can be approximated to be transversely isotropic, only five independent elastic properties instead of nine in case of orthotropic materials (independent in x, y, and z directions but symmetry about each orthogonal axis). Consequently, this approximation of transverse isotropy better substitutes the ideal scenarios of bone's anisotropy (full 21 independent elastic properties which would be derived from the generalized Hook's law) than the most frequently used assumption of isotropy (two independent elastic properties: Poisson's ratio and modulus of elasticity). For the purpose of easiness isotropic material properties are often assigned to jaw bone models. And its properties are well-thought-out uniform in all directions, unlike the human mandible material properties.

All the assigned elastic material properties may apply to bone type III and IV for this particular study are illustrated in Table 2 [54,63]. These properties ought to represent cortical bone, low density spongy bone, and high-density spongy bone. The properties given to the bone–implant transition region is developed from the properties of bulk compact and trabecular bones. Varied degree of osseointegeration are considered during this transition region. The full stability (perfect osseointegeration) is attained when the transition region has 100% bulk properties where as partial osseointegeration is said to be achieved at constant Poisson's ratio when the bulk's elastic moduli and shear moduli are described by its fractional values [61].

With respect to the bone type, the assigned elastic properties may apply to bone type II, III, or IV. Following the definition,9 the properties should represent high density cancellous bone, low density cancellous bone, and cortical bone. The properties assigned to the bone–implant transition region is acquired from the properties of bulk cortical and cancellous bones. Various degrees of osseointegeration are featured in this transition region. The assumption of perfect osseointegeration applies when the transition region has 100% bulk properties. Partial osseointegeration is represented by fractional values of the bulk's elastic and shear moduli at constant Poisson's ratio are illustrated in Table 1[54,63].

Table 1. Mechanical properties of the simulated materials [54,61].

 doi:10.20944/preprints202408.2180.v1

Properties	High density cancellous bone				Low density cancellous bone				Cortical bone			
	25%	50%	75%	100%	25%	50%	75%	100%	25%	50%	75%	100%
E_x (MPa)	287	574	861	1148	57.5	115	172.5	230	3150	6300	9450	12600
E_y (MPa)	52.5	105	157.5	210	10.5	21	31.5	42	3150	6300	9450	12600
E_z (MPa)	287	574	861	1148	57.5	115	172.5	230	4850	9700	14550	19400
v_{xy}	0.05	0.05	0.05	0.05	0.05	0.05	0.05	0.05	0.3	0.3	0.3	0.3
v_{xz}	0.32	0.32	0.32	0.32	0.32	0.32	0.32	0.32	0.253	0.253	0.253	0.253
v_{yz}	0.01	0.01	0.01	0.01	0.01	0.01	0.01	0.01	0.253	0.253	0.253	0.253
G_{xy} (MPa)	17	34	51	68	3.5	7	10.5	14	1212.5	2425	3637.5	4850
G_{xz} (MPa)	108.5	217	325.5	434	21.75	43.5	65.2	87	1425	2850	4275	5700
G_{yz} (MPa)	17	34	51	68	3.5	7	10.5	14	1425	2850	4275	5700

Table 2. Bone Type according to cortical bone thickness and cancellous Bone density [54,61].

Bone type	Cortical bone thickness	Cancellous bone density
III	1 mm	High density
IV	1 mm	Low density

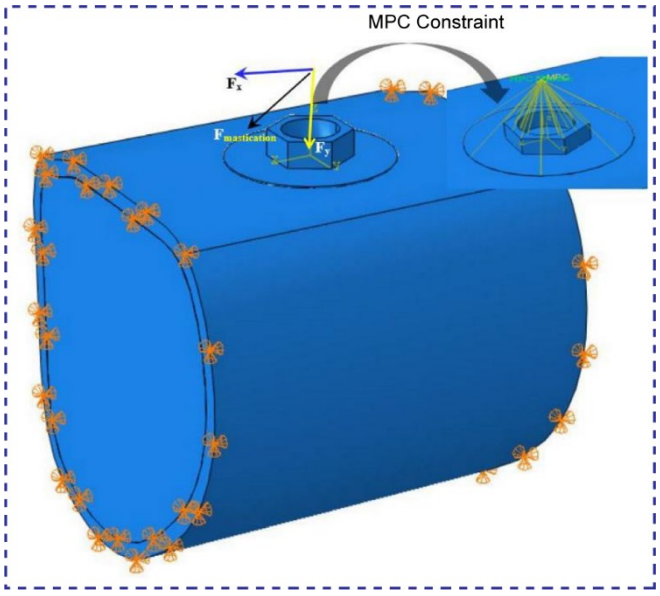

Figure 2. Assembly of short dental implant to its bone with mastication loading and BCs.

Finally, the analysis was carried out using the ABAQUS 2017 version finite element software and results were entered again in visualization and post-processing of the maps. The results were then visualized in the maximum von misses stress, principal stress and strain maps (MPa) to analyze the stress distribution in the dental implant, Spongy, and cortical bone tissue (low and high density).

2.4. FE-Mesh and Contact Definition

We used tetrahedral elements (C3D10) with linear geometric order for both the implants and the bone structures around them in a finite element (FE) meshing study of three types of short dental implants. We used a targeted meshing strategy, allocating a small element size of 0.1 mm to significant highlights such as short implants and hole regions of compact and cancellous bone. In contrast, we selected a coarser element size of 0.55 mm in the less crucial surrounding areas to maximize computing efficiency while retaining accuracy in the most important locations (refer to **Figure 3**). This method accurately models the stress and strain distributions at the bone-implant interface, which is important for checking how well the implants work mechanically when they are

 doi:10.20944/preprints202408.2180.v1

loaded in different ways. Nonlinear contact zones were defined at two critical interfaces: implant–bone, and bone-bone. Contact analysis defined the load and deformation transfer between different components. The friction coefficient (μ) was set as 0.65 for the cortical bone–implant interface [57], and 0.77 for the cancellous bone–implant interface [55].

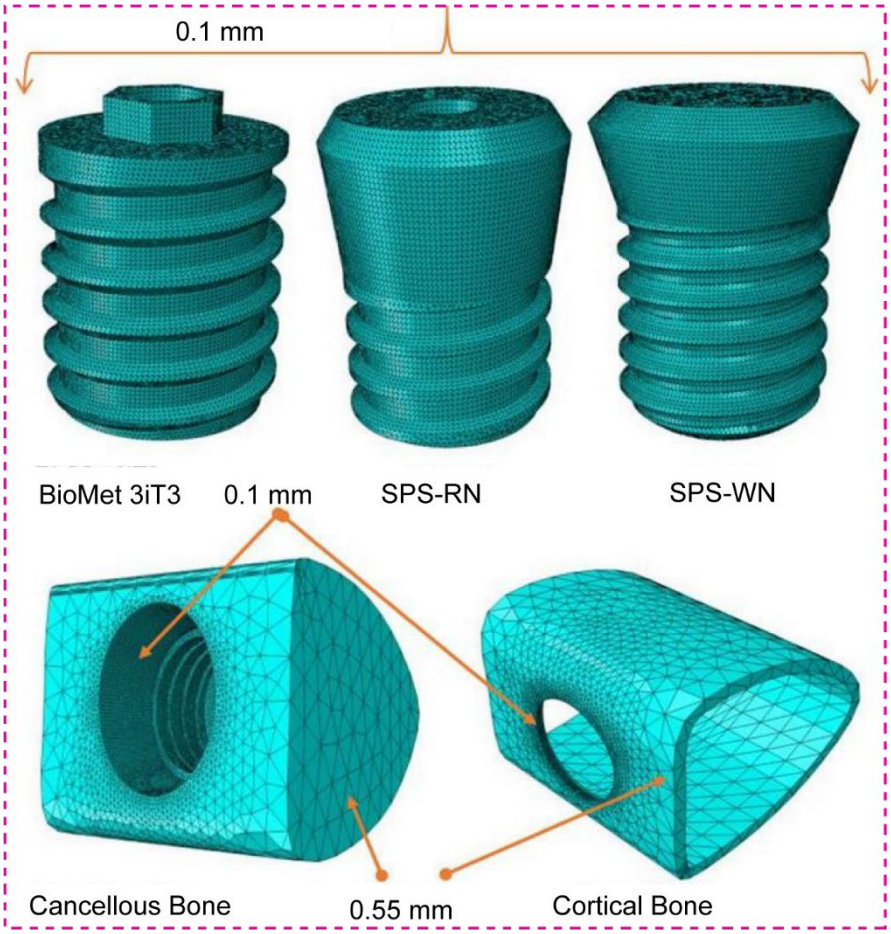

Figure 3. Finite element meshing of short dental implant and bone.

Table 3. The three short implant model Mesh statistics.

Implant Model	Implant		Cancellous bone		Cortical bone		Assembly	
	No of nodes	No of elements	No of nodes	No of elements	No of nodes	No of elements	No of nodes	No of elements
BioMet 3iT3	73,108	391,448	47,751	244,083	5,594	21,672	126,453	657,203
SPS -RN	67,363	363,525	30,876	149,142	4,974	19,015	103,213	531,682
SPS-WN	88,074	478,307	49,333	249,052	7,667	30,075	145,074	757,434

3. Results

3.1. Maximum Stress and Maximum Strain Bone

3.1.1. BioMet 3iT3 Short Implant

Table 4 shows that the mechanical response of cortical and cancellous bones varies significantly with osseointegration level. The findings demonstrate that when the osseointegration percentage in cortical bone increases from 25% to 75%, the maximum stress rises significantly from 158.4 MPa to 174.3 MPa. This implies that an improvement in bone-implant contact enhances the transmission of load to the cortical bone, leading to a rise in stress levels. Despite the increased stress, the strain inside the cortical bone reduces substantially, from 0.02559 at 25% osseointegration to 0.009997 at 75%. This

 doi:10.20944/preprints202408.2180.v1

decrease in strain suggests that the cortical bone is better able to bear applied stresses as osseointegration advances, most likely due to a more solid and durable bone-implant contact. Table 3 shows a somewhat different trend in cancellous bone. The maximum stress falls significantly as osseointegration progresses, decreasing from 19.23 MPa at 25% to 17.79 MPa at 75%. This means that the cancellous bone is under less stress when the implant integrates with the surrounding bone tissue. Similarly, strain in cancellous bone drops considerably with improved osseointegration, from 0.106 at 25% to 0.03264 at 75%. This decrease in strain demonstrates the beneficial effect of improved osseointegration on the mechanical stability of the implant, since it minimizes the risk of excessive deformation in the surrounding bone.

Table 4. Maximum stress and maximum strain for **BioMet 3iT3 Short implant** produced in bones due to applied patient biting load. With dimension of **5mm(D) x 6mm(L).**

Bone type	Osseointegeration (%)	Highest Stress		Highest Strain	
		Cortical (MPa)	Cancellous (MPa)	Cortical	Cancellous
III	25	158.4	19.23	0.02559	0.1060
	50	166.4	18.48	0.0139	0.05091
	75	174.3	17.79	0.009997	0.03264
	100	182.1	17.15	0.008047	0.02358
IV	25	303.0	18.62	0.04905	0.4088
	50	309.9	18.44	0.02379	0.2024
	75	316.2	18.36	0.01552	0.1387
	100	323.8	18.10	0.01189	0.09931

3.1.2. Standard Plus Short (SPS) Implants with Regular Neck (SRN)

The results in Table 5 show that the Standard Regular Neck SRN-Straumann® Standard Plus Short (SPS) Implants put different amounts of stress and strain on the cortical and cancellous bones at different osseointegration percentages. The findings reveal significant variations in how bone types III and IV respond to patient bite loads. When the osseointegration percentage for Bone Type III goes from 25% to 100%, the highest stress in the cortical bone changes. It goes from 137 MPa at 25% osseointegration to 136.6 MPa at 100% osseointegration. However, the maximum strain in the cortical bone drops dramatically, from 0.04126 at 25% osseointegration to 0.009295 at 100%. This suggests that with increased osseointegration, the cortical bone deforms less under strain, implying a more stable bone-implant contact. The maximum stress in type III cancellous bone decreases from 38.48 MPa at 25% osseointegration to 33.32 MPa at 100%. Similarly, the maximum strain in cancellous bone decreases significantly, from 0.1099 at 25% osseointegration to 0.02463 at 100%. These findings show that increased osseointegration not only lowers stress levels but also significantly decreases strain in cancellous bone, improving the implant's durability. For Bone Type IV, the consequences are more apparent. The maximum stress in the cortical bone is much greater, beginning at 330.1 MPa at 25% osseointegration and dropping to 300.1 MPa at 100%. The strain in the cortical bone drops significantly, from 0.08977 at 25% osseointegration to 0.02171 at 100%. These findings imply that since bone type IV is less dense, it endures more stress at first, but as osseointegration progresses, the bone's capacity to withstand deformation under load increases.

The maximum stress in type IV cancellous bone decreases significantly, from 26.12 MPa at 25% osseointegration to 25.45 MPa at 100%. The strain shows a similar trend, falling from 0.4199 at 25% osseointegration to 0.1027 at 100%. These results show that even though stress levels in cancellous bone are usually lower than those in cortical bone, the decrease in strain that comes with better osseointegration is very important for keeping the structure of the implant, especially in bone that isn't very dense.

 doi:10.20944/preprints202408.2180.v1

Table 5. Maximum stress and maximum strain for **Standard Regular neck** SRN- **Straumann® Standard Plus Short (SPS) Implants, at 4 mm long, 4.1 mm diameter** produced in bones due to applied patient biting load.

Bone type	Osseointegration (%)	Highest Stress		Highest Strain	
		Cortical (MPa)	Cancellous (MPa)	Cortical	Cancellous
III	25	137.0	38.48	0.04126	0.1099
	50	134.7	36.6	0.01988	0.05293
	75	134.1	34.88	0.01280	0.03402
	100	136.6	33.32	0.009295	0.02463
IV	25	330.1	26.12	0.08977	0.4199
	50	319.1	25.91	0.04436	0.2084
	75	311.5	25.53	0.02967	0.1393
	100	300.1	25.45	0.02171	0.1027

3.1.3. Standard Plus Short (SPS) Implants with Wide Neck (SWN)

The data in Table 6 shows that the Standard Wide Neck SWN-Straumann® Standard Plus Short (SPS) Implants, which are 4 mm long and 4.8 mm wide, cause different levels of stress and strain in the cortical and cancellous bones when the patient bites down on them. This happens at different levels of osseointegration. For bone type III, the findings reveal that when the osseointegration percentage grows from 25% to 100%, the maximum stress in the cortical bone drops from 135.5 MPa to 114.3 MPa. This tendency shows that as osseointegration develops, the implant becomes more closely integrated with the bone, prompting the cortical bone to endure less stress. As a result, the strain in the cortical bone drops substantially, from 0.04750 at 25% osseointegration to 0.009631 at 100%. This reduction in strain suggests that the bone deforms less under stress as osteointegration proceeds, which improves implant stability. The maximum stress in Type III cancellous bone decreases slightly, from 14.78 MPa at 25% osseointegration to 13.34 MPa at 100%. Similarly, the strain in cancellous bone decreases from 0.06905 at 25% to 0.01645 with 100% osseointegration. Although cancellous bone typically experiences lower stress levels than cortical bone, it also benefits from enhanced osseointegration, creating a more stable and supportive environment for the implant.

The findings for bone type IV demonstrate a more significant trend. At 25% osseointegration, the maximum stress in the cortical bone is 399.1 MPa, which decreases to 322.7 MPa at 100%. The equivalent strain in cortical bone drops significantly, from 0.09706 at 25% osseointegration to 0.02004 at 100%. This suggests that increased osseointegration significantly reduces both stress and strain in less dense Bone Type IV, which is critical for lowering the likelihood of implant failure due to excessive loading. The maximum stress in Type IV cancellous bone is relatively constant, ranging from 15.73 MPa at 25% osseointegration to 15.68 MPa at 100%. However, the strain drops significantly, from 0.2803 at 25% to 0.06946 with 100% osseointegration. This large decrease in strain indicates that with increased osseointegration, the cancellous bone is better able to distribute the applied stresses, lowering the chance of deformation and improving overall implant stability.

Table 6. Maximum stress and maximum strain for **Standard Wide Neck SWN- Straumann® Standard Plus Short (SPS) Implants, at 4 mm long, 4.8 mm** diameter produced in bones due to applied patient biting load.

Bone type	Osseointegration (%)	Highest Stress		Highest Strain	
		Cortical (MPa)	Cancellous (MPa)	Cortical	Cancellous
III	25	135.5	14.78	0.04750	0.06905
	50	127.1	14.27	0.02200	0.03396
	75	120.2	13.79	0.01368	0.02228
	100	114.3	13.34	0.009631	0.01645

 doi:10.20944/preprints202408.2180.v1

IV	25	399.1	15.73	0.09706	0.2803
	50	369.0	15.72	0.04523	0.1398
	75	344.0	15.70	0.02831	0.09292
	100	322.7	15.68	0.02004	0.06946

3.2. Maximum Shear Stresses along the Three-Plane

According to Table 7, the highest shear stresses in three planes (Sxy, Sxz, and Syz) for different implant types under a static mastication load vary significantly in cancellous and cortical bones at different stages of osseointegration.

As osseointegration grows from 25% to 100% in the BioMet 3iT3 implant model, shear stresses in cancellous bone vary to some extent. Specifically, the shear stress in the XY plane (Sxy) begins at 0.9718 MPa at 25% osseointegration and increases gradually to 1.581 MPa at 100%. The XZ and YZ planes exhibit similar tendencies, with stress levels typically increasing as osteointegration improves. Cortical bone, on the other hand, experiences more significant variations in shear stresses. For example, the shear stress in the XY plane (Sxy) rises from 97.53 MPa at 25% osseointegration to 102.8 MPa at 100%, but the XZ plane (Sxz) increases significantly from 55.37 MPa to 67.93 MPa over the same range. This suggests that when osseointegration advances, the cortical bone experiences increased shear stresses, perhaps indicating improved load transmission and stability. The shear stresses in cancellous bone in the SPS-RN (Standard Plus Regular Neck) implant model are rather consistent across varying osseointegration levels. The Sxy stress in the XY plane, for example, maintains at 1.55 MPa for all osseointegration levels. Shear stresses in cortical bone, on the other hand, fall in a clear pattern. The XY plane stress (Sxy) drops from 78.34 MPa at 25% osseointegration to 75.28 MPa at 100%. This reduction implies that when bone-implant contact improves, the distribution of shear loads becomes more uniform, possibly lowering the likelihood of localized stress concentrations. It was found that shear stresses in cancellous bone are usually lower in the SPS-WN (Standard Plus Wide Neck) implant model than in the others. The Sxy stress in the XY plane drops from 1.105 MPa at 25% osseointegration to 1.095 MPa at 100%. The cortical bone experiences a greater decrease in shear forces as osteointegration advances. For instance, the Sxy stress in the XY plane decreases from 62.77 MPa at 25% osseointegration to 57.96 MPa at 100%, with comparable trends observed in the other planes. This decrease in shear stress, especially in cortical bone, shows that the implant's stability increases with improved osseointegration, as the bone becomes more capable of handling the imposed stresses without excessive shear.

Table 7. The maximum shear stress that occur along the three-plane due to static mastication load for all three model and conditions.

Implant Model	**Osseointegeration (%)**	**Cancellous Bone**						**Cortical Bone**					
		IV			III			IV			III		
		S_{xy} (MPa)	S_{xz} (MPa)	S_{yz} (MPa)	S_{xy} (MPa)	S_{xz} (MPa)	S_{yz} (MPa)	S_{xy} (MPa)	S_{xz} (MPa)	S_{yz} (MPa)	S_{xy} (MPa)	S_{xz} (MPa)	S_{yz} (MPa)
BioMet 3iT3	25	0.9718	4.056	0.4626	1.620	6.760	0.7709	97.53	55.37	61.19	58.52	33.22	36.71
	50	1.606	6.695	0.7667	1.806	7.309	1.190	99.33	57.82	64.44	55.93	27.74	25.22
	75	1.620	6.776	0.8093	1.755	7.012	1.161	112.9	57.79	43.43	58.22	32.19	26.80
	100	1.581	6.567	0.7586	1.706	6.737	1.134	102.8	67.93	71.01	60.43	36.15	28.38
SPS -RN	25	1.552	4.733	0.9097	1.744	8.276	1.409	78.34	95.35	74.07	37.96	50.72	34.14

 doi:10.20944/preprints202408.2180.v1

	50	1.546	4.684	0.9037	1.715	7.634	1.351	77.27	95.44	73.78	39.20	50.53	35.09
	75	1.555	4.488	0.9003	1.686	7.172	1.299	77.20	96.29	74.55	40.32	50.31	36.55
	100	1.533	4.516	0.8918	1.658	7.312	1.252	75.28	95.37	75.97	41.36	50.06	37.89
SPS-WN	25	1.105	5.034	0.6854	1.266	6.566	1.039	62.77	106.9	37.46	34.44	60.75	18.85
	50	1.102	5.010	0.6851	1.242	6.306	1.014	61.05	93.30	37.13	32.98	57.03	18.83
	75	1.099	4.984	0.6847	1.219	6.064	0.9903	59.47	90.01	36.80	31.63	54.30	18.81
	100	1.095	4.961	0.6839	1.197	6.059	0.9675	57.96	59.41	36.47	30.38	51.90	18.78

S_{xy}: Shear Stresses in XY plane S_{xz}: Shear Stresses in XZ plane S_{yz}: Shear Stresses in YZ.

3.3. Maximum von Mises Stress at the Bone-Implant Contact (BIC)

For three types of short implants—BioMet 3iT3, SPS-WN, and SPS-RN—at different stages of osseointegration, Figure 4 below shows the highest von Mises stress at the bone-implant contact (BIC) area. This is the area where the bone hole meets the implant's angled neck. The black dotted circles in the illustrations represent the highest stress position in the associated contour plots.

Preprints.org (www.preprints.org) | NOT PEER-REVIEWED | Posted: 29 August 2024 doi:10.20944/preprints202408.2180.v1

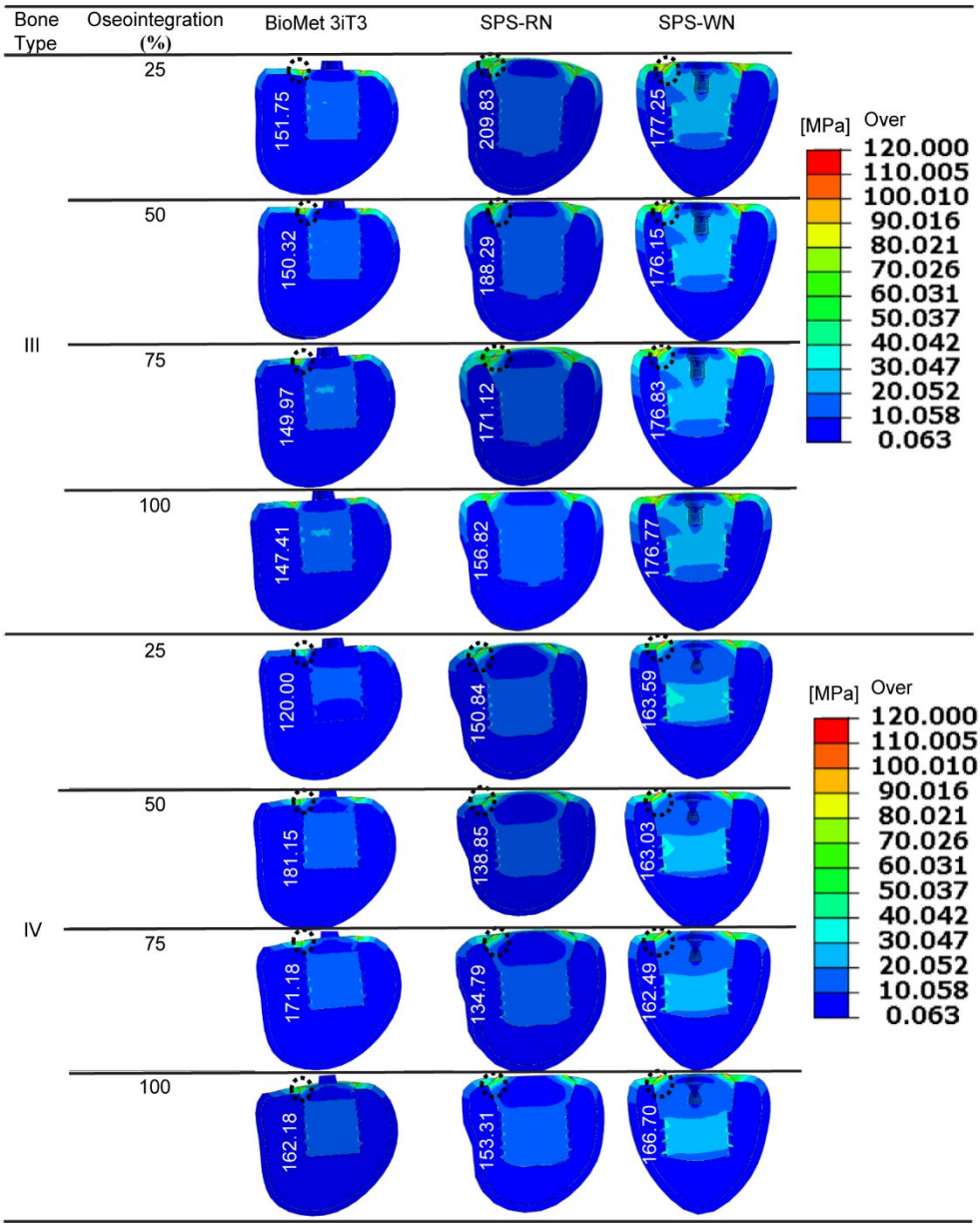

Figure 4. Highest von Mises Stress at the bone-implant contact (BIC) area for BioMet 3iT3, SPS-WN, and SPS-RN short implants at various stages of osseointegration, indicated by black dotted circles in the contour plots.

For all implant types, including Bone Type III, the maximum von Mises stress values decrease as osseointegration increases. For example, the BioMet 3iT3 implant experiences a stress drop from 151.75 MPa at 25% osseointegration to 147.41 MPa at 100% osseointegration. The SPS-WN implant exhibits a greater reduction in stress, from 209.83 MPa at 25% osseointegration to 156.82 MPa at 100%. Similarly, the SPS-RN implant experiences a slight drop from 177.25 MPa to 176.77 MPa across the same range. These findings show that when osteointegration improves, the load distribution at the bone-implant interface becomes more uniform, resulting in reduced stress concentrations and perhaps increasing implant stability. In bone type IV, the pattern is more complicated. The BioMet 3iT3 implant's von Mises stress first increases from 120 MPa at 25% osseointegration to 181.15 MPa at 50%, then gradually decreases to 162.18 MPa at 100% osseointegration. The stress on the SPS-WN implant, on the other hand, drops from 183.85 MPa at 25% osseointegration to 135.31 MPa at 100%. This shows that better osseointegration lowers stress at the interface, especially in bone that isn't as dense. The SPS-RN implant had generally steady stress values of 162.49 MPa throughout various

 doi:10.20944/preprints202408.2180.v1

osseointegration phases, with a little rise to 166.7 MPa at 100% osseointegration. These findings, as seen in the following figure, emphasize the necessity of attaining perfect osseointegration to reduce stress concentrations at the bone-implant interface, possibly lowering the likelihood of implant failure and improving long-term stability. Variations in stress between implant types and bone conditions further indicate that implant design and bone quality have a considerable impact on the mechanical environment at the BIC, which is crucial for dental implant success. maximum von Mises stress

3.4. Maximum von Mises Stress in Three Types of Short Dental Implants

Contour plots of the maximum von Mises stress, representing the distribution of mechanical stress during loading, three types of short dental implants depicted in Figure 5 below.

As osseointegration advances, Bone Type III, the BioMet 3iT3 implant, exhibits a significant rise in von Mises stress, beginning at 151.55 MPa at 25% and culminating at 255.91 MPa at 75%. Interestingly, with 100% osseointegration, the stress drops significantly to 253.82 MPa. The SPS-RN implant follows a similar trajectory, with a high starting stress of 321.7 MPa at 25% osseointegration and gradually decreasing to 260.51 MPa at 100% osseointegration. However, the SPS-WN implant suffers the greatest stress values of any implant type, beginning at 422.85 MPa at 25% osseointegration and decreasing to 333.9 MPa at 100%. These findings suggest that the SPS-WN implant puts more stress on the bone around it in Bone Type III, even when osseointegration improves. This raises the possibility of implant-bone interface stress concentration. Bone Type IV: The BioMet 3iT3 implant has a high initial von Mises stress of 252.59 MPa at 25% osseointegration, which decreases significantly to 179.51 MPa at 100%. The SPS-RN implant has a more constant stress level, beginning at 217.42 MPa at 25% osseointegration and rising slightly to 220.11 MPa at 100%. The von Mises stress on the SPS-WN implant slowly goes down, from 251.37 MPa at 25% osseointegration to 182.61 MPa at 100%. This shows that this implant design benefits the most from better osseointegration in Bone Type IV, which is less dense. Overall, the von Mises stress contours show that osseointegration is crucial for lowering stress at the bone-implant contact. When osseointegration is better, implants with higher starting stress values (SPS-WN) show bigger reductions, especially in bones that aren't very thick (Type IV). These results, as shown in the contour plots, highlight the need for attaining optimum osseointegration to reduce mechanical stress and improve implant stability.

Preprints.org (www.preprints.org) | NOT PEER-REVIEWED | Posted: 29 August 2024 doi:10.20944/preprints202408.2180.v1

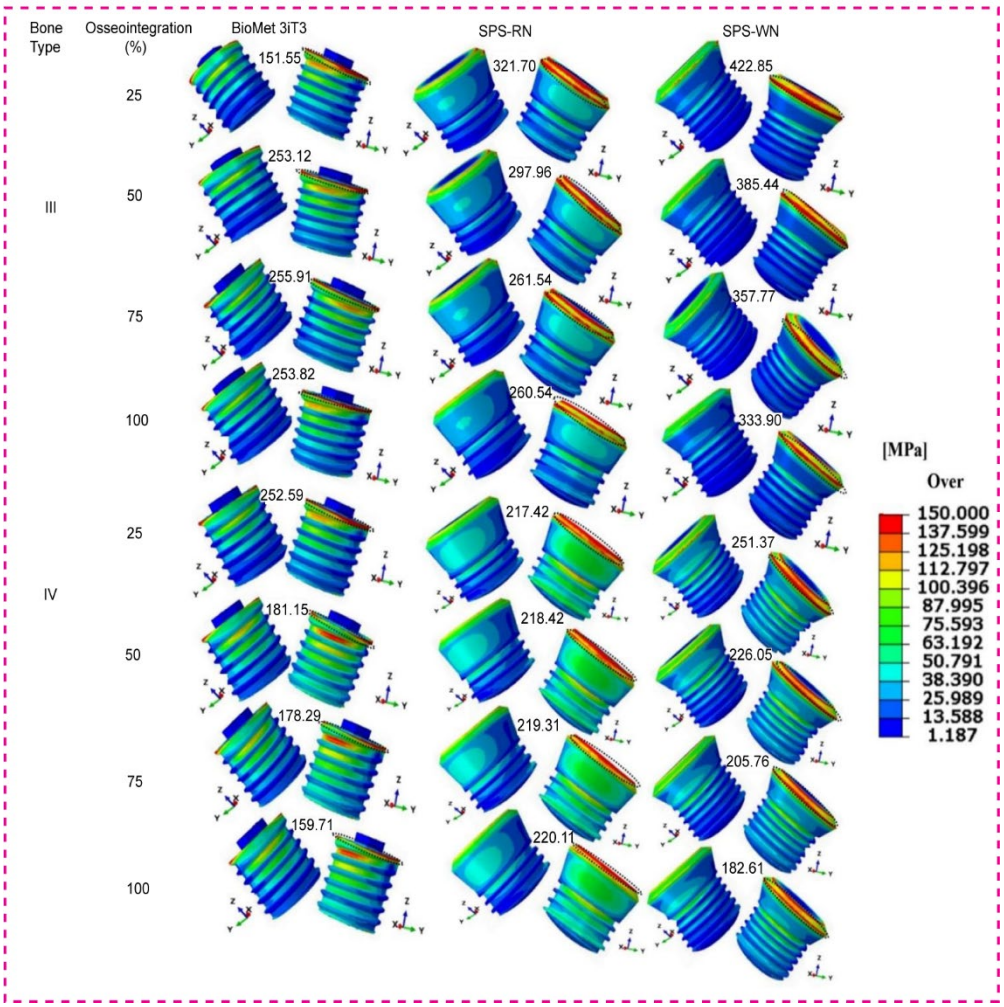

Figure 5. below shows that three types of short dental implants—BioMet 3iT3, SPS-RN, and SPS-WN—went through the highest von Mises stress at different bone types and osseointegration percentages.

When the SPS-WN implant model was used, the table shows the highest and lowest primary stresses in micrometers (μm) for low-density cancellous bone (Bone Type IV) at different levels of osseointegration (25%, 50%, 75%, and 100%). We particularly measure the strain values at the bone-implant contact interface, and the contour plots display the locations of these strains as black dotted circles. As shown in the table and contour graphs, the maximum principal strain decreases significantly as osseointegration progresses. At 25% osseointegration, the maximum strain is 280300 με, which gradually decreases to 69460 με at 100% osseointegration. This decrease in maximum strain suggests that as the bone-implant contact becomes more integrated, the bone can better distribute the load, resulting in less localized deformation. With osseointegration, the minimum principal strain decreases from 358.594 at 25% to 111.596 at 100%. This pattern demonstrates a constant increase in the implant's mechanical stability as osseointegration continues, with the bone experiencing reduced strain levels under the same loading conditions. These decreases in both maximum and lowest primary stresses indicate that establishing better osseointegration is critical for minimizing mechanical strain on the bone-implant interface, thereby improving implant stability and lifespan.

3.5. Low Density Cancellous Bone Maximum and Minimum Principal Strain

Figure 6 shows that when osseointegration happens, both the maximum and minimum principal strains for the SPS-WN implant model in low-density cancellous bone (Bone Type IV) go down by a large amount. The highest principle strain falls from 280300 at 25% osseointegration to 69460 at 100%,

 doi:10.20944/preprints202408.2180.v1

while the lowest principle strain drops from 358.594 to 111.596 across the same range. These decreases show that as the bone-implant contact becomes more integrated, the bone efficiently distributes mechanical stresses, reducing localized deformation and improving implant stability. Black dotted circles mark the positions of the highest and lowest principal strains at the implant-cancellous bone contact, illustrating key stress concentration zones.

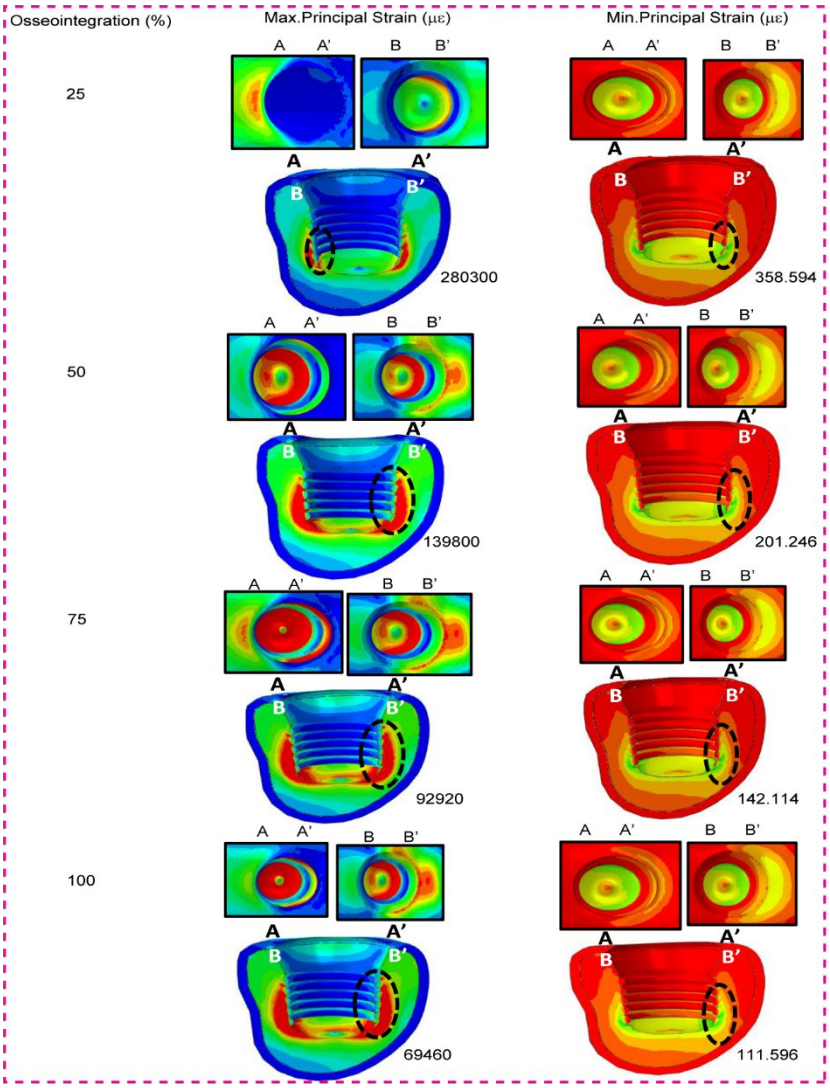

Figure 6. Low density cancellous bone maximum and minimum principal strain for 25%,50%,75%, and 100% osseointegeration of bone implant for SPS-WN implant model.

3.6. High Density Cancellous Bone Maximum and Minimum Principal Strain

As osseointegration advances, Figure 7 presented findings for the SPS-WN implant model in high-density cancellous bone (Bone Type III) demonstrate a significant reduction in both maximum and lowest principal strains. The highest main strain falls from 69050 at 25% osseointegration to 16450 at 100%, whereas the lowest principal strain drops from 157.457 to 64.1361 within the same range. These lower strains mean that as the bone-implant contact gets stronger, the bone is better able to spread mechanical stresses, which means that the implant is less likely to deform in one place and is more stable overall. Black dotted circles at the implant-cancellous bone contact depict the highest and lowest principal strains, highlighting key stress concentration locations. The contour plots further demonstrate this tendency, showing a more equal strain distribution throughout the top surface of the bone holes (A-A′ and B-B′) as osseointegration improves, which is critical for the implant's durability.

Preprints.org (www.preprints.org) | NOT PEER-REVIEWED | Posted: 29 August 2024 doi:10.20944/preprints202408.2180.v1

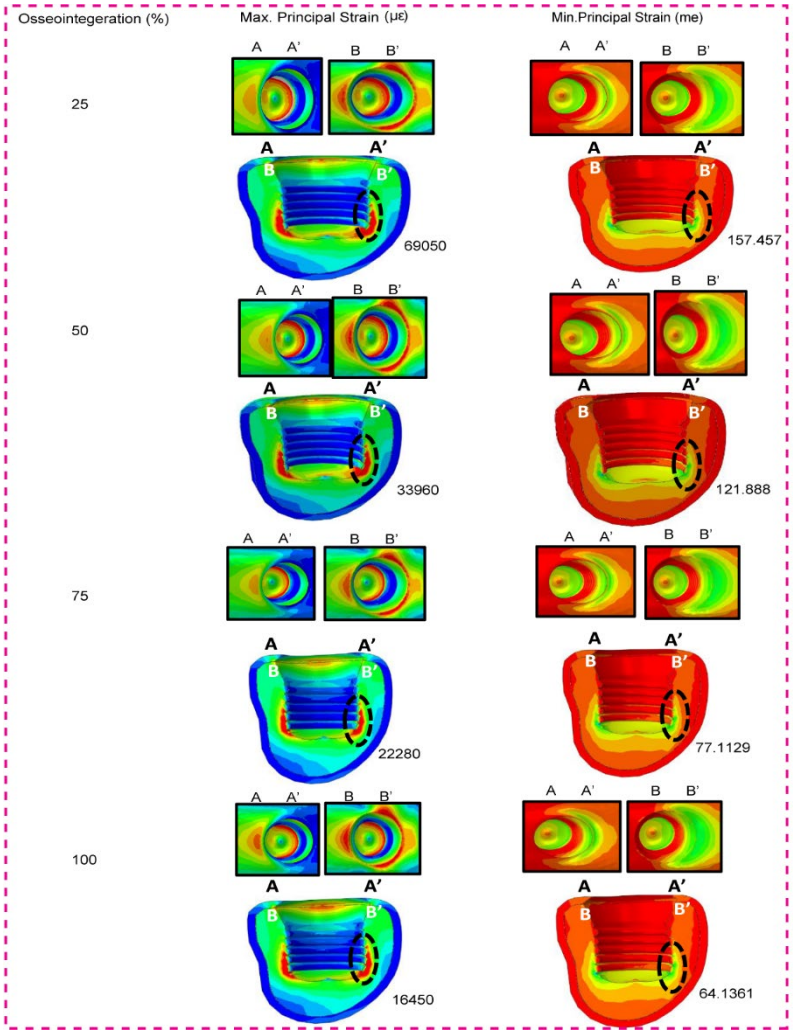

Figure 7. High density cancellous bone maximum and minimum principal strain for 25%,50%,75%, and 100% osseointegeration of bone implant for SPS-WN implant model.

3.7. Low- and High-Density Cancellous Bone Maximum and Minimum Principal Strain in Three Types of Short Dental Implants

Figure 8a shows the bar chart for maximum principal strain in low-density cancellous bone (Bone Type IV) for the BioMet 3iT3, SPS-RN, and SPS-WN implant types at four different levels of osseointegration: 25%, 50%, 75%, and 100%.We can see the highest principal strain values for low-density cancellous bone (Bone Type IV) at different osseointegration levels (25%, 50%, 75%, and 100%) for three implant models below. These are BioMet 3iT3, SPS-RN, and SPS-WN. The bar chart, which originally depicted these comparisons, generated these figures.

At 25% osseointegration, the SPS-RN implant model has the greatest maximum principal strain (419862 με), followed closely by the BioMet 3iT3 model (408801 με). At this early stage of osseointegration, the SPS-WN implant had a significantly reduced strain of 280000 με. As osteointegration progresses to 50%, 75%, and 100%, all three implant models show a significant decrease in maximum principal strain, with the SPS-WN model consistently having the lowest strain values at each stage. At 100% osseointegration, the SPS-WN model has the lowest maximum principal strain of 69000 με, suggesting a significant increase in mechanical stability when the implant completely integrates with the bone. The results, shown in the bar chart, show that the SPS-WN model is better at reducing strain at higher levels of osseointegration, especially when there is 100% bone-implant contact. The SPS-RN model experiences the most strain when osseointegration is low. This decrease in stress as osseointegration progresses underscores the need for complete integration for the implant's long-term stability and success.

 doi:10.20944/preprints202408.2180.v1

The data in Figure 8b show a considerable decrease in minimum principal strain in low-density cancellous bone (Bone Type IV) across the BioMet 3iT3, SPS-RN, and SPS-WN implant models as osseointegration advances from 25% to 100%. The SPS-WN model consistently has the lowest minimum principal strain, ranging from 280000 at 25% osseointegration to 69000 at 100%, indicating improved mechanical stability. While the BioMet 3iT3 and SPS-RN models have higher strain values throughout the osseointegration process, the highest strains were seen at the lowest levels of osseointegration. This shows how important it is to achieve full osseointegration to lower mechanical stress and improve the long-term success of the implant.

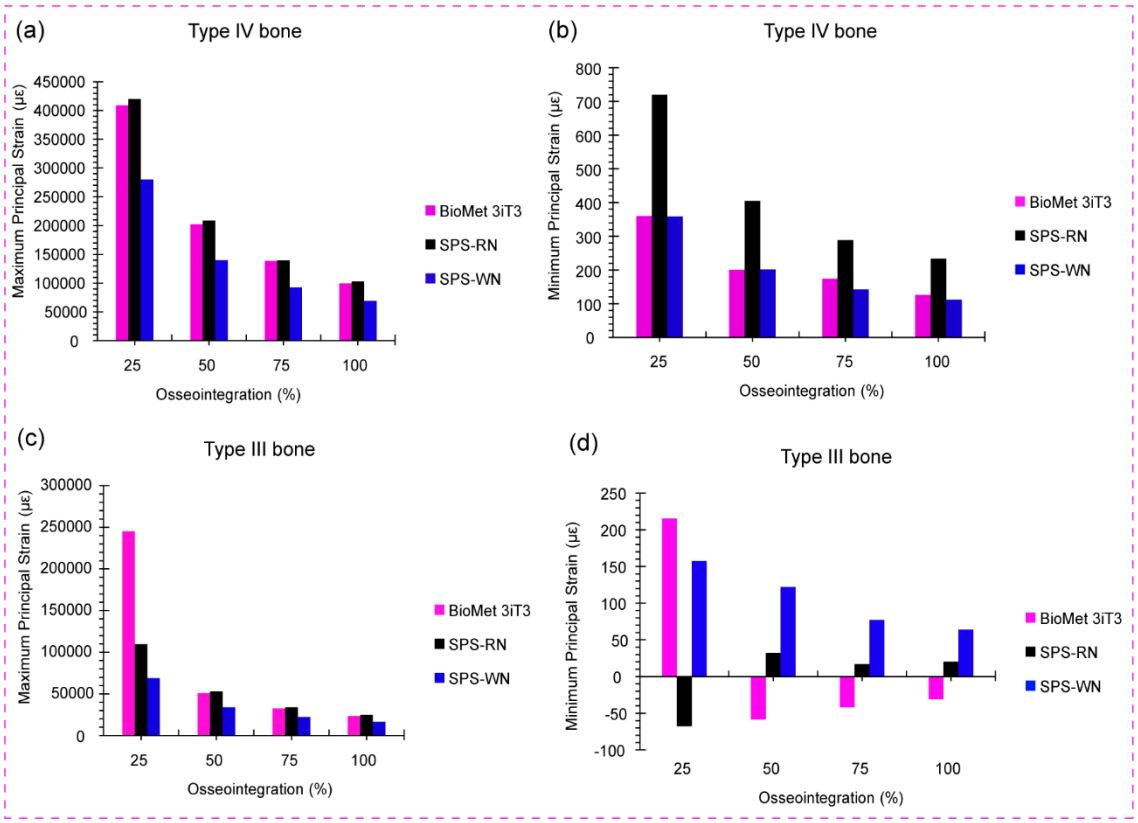

Figure 8. Shows (a) the maximum Principal Strain for type IV bone, (b)) the minimum Principal Strain for type IV bone, (c) the maximum Principal Strain for type III bone, and (d) the minimum Principal Strain for type IV bone, in the BioMet 3iT3, SPS-RN, and SPS-WN implant models for varied percentage of osseointegeration such as 25%, 50%, 75%, and 100%.

There are four levels of osseointegration shown in Figure 8c. These levels are 25%, 50%, 75%, and 100%. The graph shows the maximum principal strain in high-density cancellous bone (Bone Type III) for the BioMet 3iT3, SPS-RN, and SPS-WN implant types. At 25% osseointegration, the BioMet 3iT3 implant model had the largest maximum principal strain, reaching 245281 με. This is much larger than the strains reported in the SPS-RN and SPS-WN models, which were 109945 με and 69000 με, respectively. As osseointegration progresses, all three implant types exhibit a significant decrease in maximum principal strain. At 100% osseointegration, the BioMet 3iT3 model strain drops to 23581.7 με, whereas the SPS-RN and SPS-WN models have even lower strain values of 24633.1 με and 16446.6 με, respectively. Notably, the SPS-WN model always has the lowest maximum principal strain across all levels of osteointegration. This shows that it works better at reducing strain at the bone-implant interface as osteointegration progresses.

4. Discussion

In the setting of dental implants, the results in Table 4 show how important osseointegration is for the mechanical behavior of both cortical and cancellous bones. As osseointegration levels in

 doi:10.20944/preprints202408.2180.v1

cortical bone grow from 25% to 75%, maximum stress rises significantly from 158.4 MPa to 174.3 MPa. This increase in stress shows that improved bone-implant contact increases the efficiency of load transmission to the cortical bone, resulting in greater stress levels. However, the concurrent decrease in strain, from 0.02559 to 0.009997, suggests that the cortical bone becomes better capable of withstanding these loads without substantial deformation. This study implies that increased osseointegration not only strengthens the bone-implant interface, but also increases cortical bone load-bearing capability, most likely due to the formation of a more robust and lasting contact surface. Table 3 depicts the mechanical reaction of cancellous bone, which differs from that of other bone types. As osseointegration improves, the maximum stress decreases, from 19.23 MPa at 25% to 17.79 MPa at 75%. This decrease in stress means that as the implant becomes more integrated with the surrounding cancellous bone, the bone experiences reduced stress levels, potentially lowering the risk of stress-induced bone resorption. Furthermore, the considerable reduction in strain from 0.106 to 0.03264 suggests that better osseointegration improves the mechanical stability of the cancellous bone by reducing the danger of excessive deformation.

These results have profound implications for the use of dental implants. Increasing osseointegration leads to more even load distribution and less strain in both the cortical and cancellous bones. This means that achieving high levels of osseointegration is essential for dental implants to last and work well in the long term. In clinical practice, this underlines the significance of surgical methods and implant surface treatments that promote rapid and successful osseointegration. By maximizing bone-implant contact, physicians may guarantee that implants can resist functional stresses, lower the risk of implant failure, and improve patient outcomes in restorative dentistry.

The results in Table 5 show how important osseointegration is for controlling how the cortical and cancellous bones react to the stresses put on them by Standard Regular Neck SRN-Straumann® Standard Plus Short (SPS) Implants. As osseointegration increases from 25% to 100% in Bone Type III, the maximum stress in the cortical bone stays generally consistent, slightly dropping from 137 MPa to 136.6 MPa. However, there is a considerable decrease in strain, from 0.04126 to 0.009295, demonstrating that with improved osseointegration, the cortical bone deforms considerably less under stress. This demonstrates that improved bone-implant contact not only stabilizes the interface, but also enables the cortical bone to withstand applied stresses more efficiently without significant deformation. As osseointegration improves, the maximum stress in cancellous bone drops from 38.48 MPa to 33.32 MPa, resulting in a considerable decrease in strain from 0.1099 to 0.02463. This trend shows that enhanced osseointegration not only decreases mechanical stress on cancellous bone, but it also improves structural stability by reducing deformation.

The benefits are much more obvious for Bone Type IV, which is less dense and exposed to increased stress levels from the start. The maximum stress in cortical bone reduces substantially, from 330.1 MPa at 25% osseointegration to 300.1 MPa at 100%. Meanwhile, the strain in cortical bone decreases from 0.08977 to 0.02171, indicating that the bone's capacity to resist deformation improves with osseointegration. In cancellous bone, the maximum stress reduces at least from 26.12 MPa to 25.45 MPa, whereas strain decreases significantly from 0.4199 to 0.1027. These results show that even though cancellous bone is under less stress than cortical bone, the decrease in stress that comes with better osseointegration is very important for keeping the implant's structure, especially in bone types that aren't very dense.

These findings highlight the necessity of establishing optimum osseointegration in dental implant treatments, especially when working with less dense bone types such as Bone Type IV. The observed decrease in strain and stress levels with enhanced osseointegration indicate that improving bone-implant contact is critical for long-term implant stability and longevity. Clinically, this emphasizes the need for precise surgical methods and implant surfaces that promote quick and successful osseointegration. By providing strong and stable bone-implant interfaces, clinicians may lower the chance of implant failure, especially in difficult instances when bone density is limited, hence enhancing patient outcomes and implant life.

 doi:10.20944/preprints202408.2180.v1

The stress and strain responses of the cortical and cancellous bones change a lot at different levels of osseointegration for the Standard Wide Neck SWN-Straumann® Standard Plus Short (SPS) Implants, as shown in Table 6. For Bone Type III, the highest stress in the cortical bone drops from 135.5 MPa to 114.3 MPa as osseointegration goes from 25% to 100%. This shows that better bone-implant contact lowers stress levels in the cortical bone. In addition, there is a significant decrease in strain from 0.04750 to 0.009631, indicating that as osseointegration advances, the cortical bone deforms less, improving implant stability. The maximum stress in cancellous bone drops at least from 14.78 MPa to 13.34 MPa, while strain also decreases from 0.06905 to 0.01645. Although cancellous bone experiences less stress than cortical bone, the decreased strain caused by enhanced osseointegration implies a more stable and supportive environment for the implant.

In Bone Type IV, the pattern is more noticeable. At 25% osseointegration, the maximum stress in cortical bone begins at 399.1 MPa and reduces to 322.7 MPa at 100% osseointegration. The related strain likewise drops substantially, from 0.09706 to 0.02004. These results emphasize the importance of osseointegration in reducing stress and strain in less dense Bone Type IV, which is critical for minimizing the likelihood of implant failure due to overloading. The maximum stress in cancellous bone stays rather constant, ranging from 15.73 MPa to 15.68 MPa, whereas strain decreases significantly from 0.2803 to 0.06946 as osseointegration improves. This large reduction in strain highlights cancellous bone's superior capacity to disperse applied stresses, reducing deformation and contributing to implant durability.

These findings highlight the importance of obtaining excellent osseointegration in maintaining mechanical stability and success with dental implants. For denser bone types, such as Type III, enhanced osseointegration decreases both stress and strain, resulting in better load distribution and less bone deformation. In less dense bone types, such as Type IV, where higher initial stress and strain values increase the likelihood of implant failure, enhanced osseointegration is even more important. In terms of clinical practice, this emphasizes how crucial it is to choose implant configurations and surgical methods that facilitate efficient osseointegration, especially in patients with reduced bone density. By achieving these conditions, we can significantly reduce the stress on the surrounding bone, thereby enhancing implant longevity and enhancing patient outcomes in restorative dentistry.

When osseointegration goes from 25% to 100%, Table 7 shows the changes in shear stress in three planes (Sxy, Sxz, and Syz) for different types of implants in cancellous and cortical bones. The stresses are caused by static mastication. In the BioMet 3iT3 implant model, the cancellous bone shear stresses rise over time. This is especially true in the XY plane (Sxy), where the stresses rise from 0.9718 MPa at 25% osseointegration to 1.581 MPa at 100%. The XZ and YZ planes replicate this pattern, showing that an improvement in osseointegration leads to slightly higher shear stresses in the cancellous bone, possibly because of enhanced load transfer through the implant. Cortical bone in the BioMet 3iT3 model exhibits more noticeable shear stress changes, with considerable increases seen, particularly in the XZ plane (Sxz), where stress rises from 55.37 MPa to 67.93 MPa. These results suggest that better osseointegration leads to better load distribution in the cortical bone. This creates more shear stress, which could mean that the bone-implant contact is more stable and effective. In the SPS-RN (Standard Plus Regular Neck) implant model, shear stresses in cancellous bone stay about the same at all osseointegration levels. The Sxy stress in the XY plane stays at about 1.55 MPa. But as osseointegration goes up, shear stress in cortical bone goes down a lot. This is especially true in the XY plane, where stress drops from 78.34 MPa at 25% osseointegration to 75.28 MPa at 100%. This means that as osseointegration gets better, the shear stresses in the cortical bone become more evenly distributed. This makes it less likely that there will be localized stress concentrations that could weaken the implant's durability. In the SPS-WN (Standard Plus Wide Neck) implant model, shear stresses in cancellous bone are often lower than in the other models. As osseointegration progresses, only small decreases are seen. The Sxy stress in the XY plane drops slightly, from 1.105 MPa at 25% osseointegration to 1.095 MPa at 100%. The cortical bone experiences the most significant changes as osseointegration progresses, particularly in the XY plane, where the Sxy stress decreases from 62.77 MPa to 57.96 MPa. This lower level of shear stress in cortical bone suggests that as osseointegration

 doi:10.20944/preprints202408.2180.v1

gets better, the bone gets better at handling stresses. This makes implants more stable by lowering the risk of bone damage caused by shear.

These findings highlight the need for enhancing osseointegration to increase the mechanical stability of dental implants. The increase in shear stress in cortical bone found in the BioMet 3iT3 model promotes enhanced load distribution and implant stability, especially when osseointegration improves the bone-implant interaction. In contrast, the steady or decreasing shear stresses found in the SPS-RN and SPS-WN models suggest that enhanced osseointegration results in a more uniform distribution of loads, lowering the risk of localized shear stress concentrations that might possibly compromise the bone or implant. Clinically, our results highlight the need for implant designs and surface treatments that promote quick and robust osseointegration, especially for individuals with varied bone densities, to assure long-term implant success and durability.

Figure 4 shows how important osseointegration is for changing the biomechanical environment at the bone-implant contact (BIC) region, especially when von Mises stress is present. As osseointegration gets better across all implant types and bone conditions, the highest von Mises stress at the BIC goes down. This means that the load is spread out more evenly and there are fewer stress concentrations. This is especially visible in the SPS-WN implant, which shows a considerable decrease in stress from 209.83 MPa at 25% osseointegration to 156.82 MPa at 100%. Such a reduction in stress concentration is critical for improving the implant's mechanical stability because it reduces the danger of localized bone resorption and implant failure caused by excessive stress. The findings are more complicated for bone type IV, which is less dense and more prone to mechanical failure. The first rise in von Mises stress in the BioMet 3iT3 implant model at 50% osseointegration and then the subsequent fall shows that the bone-implant contact changes as osseointegration progresses. This adaptability is significant in less dense bones because stress distribution may be unequal, making excellent osseointegration even more important for implant life. The fact that the SPS-RN implant's stress levels stayed the same during different stages of osteointegration shows how important implant design is for maintaining consistent biomechanical function. This stability may lead to decreased mechanical problems over time, especially in clinical settings where bone quality fluctuates.

The results underline the importance of obtaining optimum osseointegration for the mechanical success of dental implants. Improved osseointegration lowers stress concentrations at the BIC, increasing implant durability and decreasing the likelihood of failure. This stresses the necessity of choosing implants with designs that facilitate consistent stress distribution, especially in individuals with reduced bone density (e.g., Type IV bone). Furthermore, the findings suggest that we can create personalized implant designs to enhance stress distribution for different bone types, thereby improving dental implantology outcomes. These findings underscore the need for patient-specific techniques in implant dentistry, where the unique biomechanical environment of each patient's bone structure guides implant selection and placement procedures, within the broader context of biomechanics.

Figure 5 displays contour plots that demonstrate the biomechanical value of osseointegration in dental implants, particularly in lowering von Mises stress at the bone-implant contact. For Bone Type III, both the BioMet 3iT3 and SPS-RN implants show less stress as osseointegration improves. This means that the load is better distributed, and there is a lower chance of localized bone fractures. However, despite a considerable decrease, the SPS-WN implant still imposes higher stress levels, suggesting potential stress concentration hazards at the bone-implant interface, especially in denser bone types. In Bone Type IV, which is less dense, all implant types show a big drop in von Mises stress as osseointegration happens. The SPS-WN implant benefits the most from better osseointegration. This shows that adequate osseointegration is critical for improving the biomechanical stability of implants, particularly in less dense bones where implant failure is more likely. Also, the fact that both maximum and minimum principal strains go down as osseointegration gets better makes it even more important to make sure that the bone and implant have a strong contact. As strain decreases, the bone's capacity to uniformly distribute stresses increases, reducing localized deformation and increasing implant lifetime. These findings highlight the need for adequate

 doi:10.20944/preprints202408.2180.v1

osseointegration in clinical applications to increase mechanical stability and the long-term success of dental implants, particularly in unfavorable bone scenarios.

The findings in Figure 6 show a considerable decrease in both maximum and minimum principal strains in low-density cancellous bone (Bone Type IV) as osseointegration improves in the SPS-WN implant model. This significant reduction in strain suggests that improved osseointegration causes more efficient load distribution at the bone-implant interface, minimizing localized deformation and enhancing overall implant stability. The black dotted dots showing the significant stress concentration zones underline the essential places where osseointegration plays an important role in reducing mechanical strain, which is necessary for the lifetime and effectiveness of dental implants in biomechanical applications. This highlights the significance of obtaining optimum osseointegration, especially in low-density bone, in improving the mechanical performance and longevity of dental implants.

Figure 7 shows that the maximum and lowest principal strains in the SPS-WN implant model for high-density cancellous bone (Bone Type III) decrease significantly as osseointegration develops. This decrease in strain indicates the bone's enhanced ability to distribute mechanical stresses efficiently, lowering the risk of localized deformation and improving the implant's overall stability. The black dotted dots represent the greatest and lowest main stresses at the implant-cancellous bone contact, highlighting significant stress concentration locations. The contour plots provide evidence of a more uniform strain distribution, which strengthens the biomechanical benefit of greater osseointegration. This is important because long-term durability and clinical implant success depend on improved osseointegration.

The findings in Figure 8a demonstrate the importance of osseointegration in lowering the maximum principal strain in low-density cancellous bone (Bone Type IV) across three implant models: BioMet 3iT3, SPS-RN, and SPS-WN. When it came to 25% osseointegration, the SPS-RN implant had the most strain, which means it had a higher chance of deforming locally and failing biomechanically in the early stages of integration. The SPS-WN model regularly demonstrates the lowest strain values, especially at 100% osseointegration, when the strain lowers significantly to 69000 με. This shows that as osseointegration improves, the SPS-WN implant design becomes more successful at reducing strain and increasing mechanical stability, making it ideal for long-term implant success. The fact that strain went down as osseointegration went up across all models shows how important it is to get total bone-implant integration to improve load distribution, reduce mechanical stress, and make implants last longer and work better in clinical settings.

The results in Figure 8b emphasize the critical need to achieve complete osseointegration in low-density cancellous bone (Bone Type IV) to improve implant stability. The SPS-WN implant model has a much lower minimum principal strain, especially as osseointegration increases from 25% to 100%. This shows that it can spread mechanical loads more evenly, which lowers localized stress and the chance of bone resorption. The BioMet 3iT3 and SPS-RN models, on the other hand, had higher strain values, especially at lower levels of osseointegration. This showed how biomechanically weak implants can be when they don't integrate properly. These findings suggest that maximizing osseointegration is critical for reducing mechanical strain at the bone-implant interface, which is critical for the long-term durability and effectiveness of dental implants in clinical settings.

Figure 8c shows that the SPS-WN implant model is better for biomechanics in high-density cancellous bone (Bone Type III), since it always shows the lowest maximum principal strain at all levels of osseointegration. This shows better load distribution and lower mechanical stress at the bone-implant contact, which is important for reducing the risk of localized bone damage and improving implant stability. The considerable decrease in strain reported across all implant types as osseointegration builds demonstrates the need for complete integration to maintain excellent biomechanical function. The BioMet 3iT3 model, despite initially displaying the greatest strain, gains significantly from increased osseointegration; nonetheless, the SPS-WN model's continuously lower strain shows that its design is more successful in reducing stress and increasing long-term implant success in clinical applications.

 doi:10.20944/preprints202408.2180.v1

The results shown in Figure 8d demonstrate the importance of osseointegration in reducing the minimum principal strain in high-density cancellous bone (Bone Type III) across various implant types. The BioMet 3iT3 model initially shows the greatest strain at 25% osseointegration, suggesting a higher risk of localized bone stress. However, as osseointegration advances, all models show a notable drop in strain. The SPS-WN model has the most dramatic reduction, particularly at 75% osseointegration, when it records the lowest strain value of 16.985 με. This demonstrates that the SPS-WN implant is highly effective at lowering mechanical stress at the bone-implant interface, which improves implant stability and reduces the risk of bone destruction. The continued decline in strain with increasing osseointegration highlights the necessity of complete integration for the long-term biomechanical success of dental implants, especially in high-density bone.

5. Conclusions

This research examines the biomechanical performance of three kinds of short dental implants—BioMet 3iT3, SPS-RN, and SPS-WN—through four phases of osseointegration (25%, 50%, 75%, and 100%) in cancellous bones with high and low densities (Bone Type III and IV, respectively). The following summaries are based on the current research.

- Osseointegration Improves Implant Stability: Across all implant types and bone densities, increasing osseointegration results in a substantial decrease in both von Mises stress and principal strains at the bone-implant interface, indicating better load distribution and a reduced likelihood of localized destruction of the bone.
- The SPS-WN implant exhibits superior biomechanical performance, with the lowest maximum and minimum principal strains at all phases of osseointegration, particularly at 100% integration. This shows that the SPS-WN implant design is more successful at reducing mechanical stress while increasing stability, making it ideal for individuals with variable bone densities.
- The Effect of Bone Density on Stress Distribution: All implants showed higher initial stress and strain in low-density cancellous bone (Bone Type IV). This shows how important it is to achieve complete osseointegration to reduce these effects. The SPS-WN implant was particularly successful in lowering stress in low-density bone, indicating its potential for use in patients with poor bone quality.
- BioMet 3iT3 Implant Needs Careful Consideration: The BioMet 3iT3 implant had greater starting strain values, but it benefitted from enhanced osseointegration, resulting in considerable stress and strain reductions. However, the fact that it consistently shows higher strain values than the SPS-WN model suggests that it might not work as well when bone quality is low or osseointegration is weak.
- Critical Role of Complete Osseointegration: The research emphasizes the need for 100% osseointegration for proper implant function. Incomplete osseointegration is linked to increased stress concentrations and a higher likelihood of implant failure, especially in less dense bones.

In conclusion, this research highlights the significance of implant design and osseointegration in assuring mechanical stability and long-term success of dental implants. The SPS-WN implant type is the most biomechanically advantageous, especially in complicated bone conditions, making it an excellent choice for clinical applications requiring excellent osseointegration.

Author Contributions: Conceptualization, D.B.A, M.T, and S.J-H.; methodology, D.B.A, S.J-H, and M.T.; software, D.B.A, M.T, and S.J-H.; validation, D.B.A,S.J-H. and M.T.; formal analysis, D.B.A.; investigation, D.B.A.; data curation, D.B.A,; writing—original draft preparation, D.B.A ; writing—review and editing, D.B.A., M.T., S.J-H.; supervision, M.T. and S.J.H; project administration, S.J-H and M.T. All authors have read and agreed to the published version of the manuscript.

Funding: This research was funded by the National Science and Technology Council (Taiwan) the Ministry of Science and Technology of Taiwan (project No. 111-2221-E-011 -096 -MY3MOST-105-2221-E-011-058-MY2) and partially supported by MEXT Grant-in-Aid for Scientific Research (A) (Grant No. 21H04731).

Data Availability Statement: Not applicable.

 doi:10.20944/preprints202408.2180.v1

Acknowledgments: The authors acknowledge the use of the language editing software QuillBot (https://quillbot.com/) for enhancing grammar, spelling, paraphrasing, and plagiarism checking.

Conflicts of Interest: The authors declare no conflict of interest.

References

1. Rane, A.V.; Abitha, V.K.; Sisanth, K.S.; Kanny, K. Introduction to Polymer Materials for Implants. In *Polymeric Materials for Biomedical Implants*; Elsevier, 2024; pp. 1–29.
2. Upadhyay, A.; Pradhan, L.; Yenurkar, D.; Kumar, K.; Mukherjee, S. Advancement in Ceramic Biomaterials for Dental Implants. *Int. J. Appl. Ceram. Technol.* **2024**, *21*, 2796–2817.
3. Alfaraj, T.A.; Al-Madani, S.; Alqahtani, N.S.; Almohammadi, A.A.; Alqahtani, A.M.; AlQabbani, H.S.; Bajunaid, M.K.; Alharthy, B.A.; Aljalfan, N. Optimizing Osseointegration in Dental Implantology: A Cross-Disciplinary Review of Current and Emerging Strategies. *Cureus* **2023**, *15*.
4. Ćelić, R.; Pezo, H.; Senzel, S.; Ćelić, G. The Relationship between Dental Occlusion and "Prosthetic Occlusion" of Prosthetic Restorations Supported by Natural Teeth and Osseointegrated Dental Implants. In *Human Teeth-From Function to Esthetics*; IntechOpen, 2023 ISBN 1837686599.
5. Michalakis, K.; Misci, S.; Abdallah, A.; Vasilaki, D.; Hirayama, H. Implant Supportive Maintenance for Fixed Prosthetic Rehabilitations: The Patient with the Complete Arch Fixed Implant–Supported Rehabilitation: Prosthetic Concepts to Optimize Maintenance Protocols. *Sav. Dent. Implant.* **2024**, 357–380.
6. Xu, X.; Zuo, J.; Zeng, H.; Zhao, Y.; Fan, Z. Improving Osseointegration Potential of 3D Printed PEEK Implants with Biomimetic Periodontal Ligament Fiber Hydrogel Surface Modifications. *Adv. Funct. Mater.* **2024**, *34*, 2308811.
7. Tari, S.R.; Gehrke, S.A.; Scarano, A.; Di Palma, G.; Scarano, P.; Scarano, A.; Dei Vestini, V. Immediately Loaded Mini Dental Implants as Overdenture Retainers: Histomorphometric Analysis of Implant Retrieved from Man. *Ann. Stomatol.* **2024**, *2*, 1–4.
8. Shrivas, S.; Samaur, H.; Yadav, V.; Boda, S.K. Soft and Hard Tissue Integration around Percutaneous Bone-Anchored Titanium Prostheses: Toward Achieving Holistic Biointegration. *ACS Biomater. Sci. Eng.* **2024**, *10*, 1966–1987.
9. Trombelli, L.; Farina, R.; Tomasi, C.; Vignoletti, F.; Paolantoni, G.; Giordano, F.; Ortensi, L.; Simonelli, A. Factors Affecting Radiographic Marginal Bone Resorption at Dental Implants in Function for at Least 5 Years: A Multicenter Retrospective Study. *Clin. Oral Implants Res.* **2024**.
10. Emfietzoglou, R.; Dereka, X. Survival Rates of Short Dental Implants (≤ 6 Mm) Used as an Alternative to Longer (> 6 Mm) Implants for the Rehabilitation of Posterior Partial Edentulism: A Systematic Review of RCTs. *Dent. J.* **2024**, *12*, 185.
11. de Araújo Nobre, M.; Antunes, C.; Lopes, A.; Ferro, A.; Nunes, M.; Gouveia, M.; Azevedo Coutinho, F.; Salvado, F. Partial Implant Rehabilitations in the Posterior Regions of the Jaws Supported by Short Dental Implants (7.0 Mm): A 7-Year Clinical and 5-Year Radiographical Prospective Study. *J. Clin. Med.* **2024**, *13*, 1549.
12. Scarano, A.; Khater, A.G.A.; Gehrke, S.A.; Inchingolo, F.; Tari, S.R. Animal Models for Investigating Osseointegration: An Overview of Implant Research over the Last Three Decades. *J. Funct. Biomater.* **2024**, *15*, 83.
13. Gao, J.; Pan, Y.; Gao, Y.; Pang, H.; Sun, H.; Cheng, L.; Liu, J. Research Progress on the Preparation Process and Material Structure of 3D-Printed Dental Implants and Their Clinical Applications. *Coatings* **2024**, *14*, 781.
14. Valeri, C.; Aloisio, A.; Marzo, G.; Costigliola, G.; Quinzi, V. What Is the Impact of Patient Attributes, Implant Characteristics, Surgical Techniques, and Placement Location on the Success of Orthodontic Mini-Implants in Young Adults? A Systematic Review and Meta-Analysis. *Saudi Dent. J.* **2024**.
15. Tseng, K.-F.; Shiu, S.-T.; Hung, C.-Y.; Chan, Y.-H.; Chee, T.-J.; Huang, P.-C.; Lai, P.-C.; Feng, S.-W. Osseointegration Potential Assessment of Bone Graft Materials Loaded with Mesenchymal Stem Cells in Peri-Implant Bone Defects. *Int. J. Mol. Sci.* **2024**, *25*, 862.
16. Javed, F.; Romanos, G.E. The Role of Primary Stability for Successful Immediate Loading of Dental Implants. A Literature Review. *J. Dent.* **2010**, *38*, 612–620, doi:https://doi.org/10.1016/j.jdent.2010.05.013.
17. Luo, F.; Mo, Y.; Jiang, J.; Wen, J.; Ji, Y.; Li, L.; Wan, Q. Advancements in Dental Implantology: The Alveolar Ridge Split Technique for Enhanced Osseointegration. *Clin. Implant Dent. Relat. Res.*
18. Hagberg, K.; Jahani, S.A.G.; Omar, O.; Thomsen, P. Osseointegrated Prostheses for the Rehabilitation of Patients with Transfemoral Amputations: A Prospective Ten-Year Cohort Study of Patient-Reported Outcomes and Complications. *J. Orthop. Transl.* **2023**, *38*, 56–64.
19. Donos, N.; Akcali, A.; Padhye, N.; Sculean, A.; Calciolari, E. Bone Regeneration in Implant Dentistry: Which Are the Factors Affecting the Clinical Outcome? *Periodontol. 2000* **2023**, *93*, 26–55.
20. Mohammadi, A.; Dehkordi, N.R.; Mahmoudi, S.; Rafeie, N.; Sabri, H.; Valizadeh, M.; Poorsoleiman, T.; Jafari, A.; Mokhtari, A.; Khanjarani, A. Effects of Drugs and Chemotherapeutic Agents on Dental Implant

Osseointegration: A Narrative Review. *Curr. Rev. Clin. Exp. Pharmacol. Former. Curr. Clin. Pharmacol.* **2024**, *19*, 42–60.
21. Jambhulkar, N.; Jaju, S.; Raut, A.; Bhoneja, B. A Review on Surface Modification of Dental Implants among Various Implant Materials. *Mater. Today Proc.* **2023**, *72*, 3209–3215.
22. Gulati, K.; Chopra, D.; Kocak-Oztug, N.A.; Verron, E. Fit and Forget: The Future of Dental Implant Therapy via Nanotechnology. *Adv. Drug Deliv. Rev.* **2023**, *199*, 114900.
23. Šromová, V.; Sobola, D.; Kaspar, P. A Brief Review of Bone Cell Function and Importance. *Cells* **2023**, *12*, 2576.
24. Yang, Y.; Liu, Y.; Yuan, X.; Ren, M.; Chen, X.; Luo, L.; Zheng, L.; Liu, Y. Three-Dimensional Finite Element Analysis of Stress Distribution on Short Implants with Different Bone Conditions and Osseointegration Rates. *BMC Oral Health* **2023**, *23*, 220.
25. Su, C.; Kreis, B.; Chen, K.; Glynn, P.; Hay, P.; Poerschke, D.; Schepp, B. Fucose-Dependent Differentiation and Gene Expression of Common Myeloid Progenitor Cells Through Notch Signaling Pathways. *Discussions* **2023**, *2*, 1.
26. Zdero, R.; Brzozowski, P.; Schemitsch, E.H. Biomechanical Properties of Artificial Bones Made by Sawbones: A Review. *Med. Eng. Phys.* **2023**, 104017.
27. Choukroun, E.; Parnot, M.; Surmenian, J.; Gruber, R.; Cohen, N.; Davido, N.; Simonpieri, A.; Savoldelli, C.; Afota, F.; El Mjabber, H. Bone Formation and Maintenance in Oral Surgery: The Decisive Role of the Immune System—A Narrative Review of Mechanisms and Solutions. *Bioengineering* **2024**, *11*, 191.
28. Hossain, N.; Mobarak, M.H.; Islam, M.A.; Hossain, A.; Al Mahmud, M.Z.; Rayhan, M.T.; Chowdhury, M.A. Recent Development of Dental Implant Materials, Synthesis Process, and Failure–a Review. *Results Chem.* **2023**, 101136.
29. Manfredini, M.; Poli, P.P.; Giboli, L.; Beretta, M.; Maiorana, C.; Pellegrini, M. Clinical Factors on Dental Implant Fractures: A Systematic Review. *Dent. J.* **2024**, *12*, 200.
30. Menchini-Fabris, G.B.; Toti, P.; Crespi, G.; Covani, U.; Crespi, R. Distal Displacement of Maxillary Sinus Anterior Wall versus Conventional Sinus Lift with Lateral Access: A 3-Year Retrospective Computerized Tomography Study. *Int. J. Environ. Res. Public Health* **2020**, *17*, 7199.
31. Rizvi, Z.H.; Bhangoo, H.S.; Meyer, A.J.; Rao, G. V; Buttar, N.S. Full-Thickness Endoscopic and Combined Laparoscopic-Endoscopic Techniques. In *Advanced Techniques for Endoscopic Resection in the GI Tract*; CRC Press, 2024; pp. 387–402.
32. Rajan, S.; Rishi, G.; Ibrahim, M. Opioid Alternatives in Spine Surgeries. *Curr. Opin. Anesthesiol.* **2024**, 10–1097.
33. Harky, A.; Chow, V.J.; Voller, C.; Goyal, K.; Shaw, M.; Bhawnani, A.; Kenawy, A.; Wilson, I.; Lip, G.Y.H.; Field, M. Stroke Outcomes Following Cardiac and Aortic Surgery Are Improved by the Involvement of a Stroke Team. *Eur. J. Clin. Invest.* **2024**, e14275.
34. Wu, H.-C.; Huang, H.-L.; Fuh, L.-J.; Tsai, M.-T.; Hsu, J.-T. Influence of Implant Length and Insertion Depth on Primary Stability of Short Dental Implants: An in Vitro Study of a Novel Mandibular Artificial Bone Model. *J. Dent. Sci.* **2024**, *19*, 139–147.
35. Thoma, D.S.; Haas, R.; Sporniak-Tutak, K.; Garcia, A.; Taylor, T.D.; Tutak, M.; Pohl, V.; Hämmerle, C.H.F. Randomized Controlled Multi-centre Study Comparing Shorter Dental Implants (6 Mm) to Longer Dental Implants (11–15 Mm) in Combination with Sinus Floor Elevation Procedures: 10-year Data. *J. Clin. Periodontol.* **2024**, *51*, 499–509.
36. Kaptı, Y.; Korkmaz, İ.H.; Yanıkoğlu, N. Comparison of Short Implant, Angled Implant, Distal Extension and Grafting Methods for Atrophic Maxillary Posterior Region: A Finite Element Study. *J. Med. Biol. Eng.* **2024**, *44*, 57–66.
37. Bilhan, H. The Role of the Dental Implant in Removable Partial Dentures. In *Removable Partial Dentures: A Practitioners' Manual*; Springer, 2024; pp. 223–241.
38. Hossain, N.; Islam, M.A.; Ahmed, M.M.S.; Chowdhury, M.A.; Mobarak, M.H.; Rahman, M.M.; Hossain, M.D.H. Advances and Significances of Titaniumin Dental Implant Applications. *Results Chem.* **2024**, 101394.
39. Marasli, C.; Katifelis, H.; Gazouli, M.; Lagopati, N. Nano-Based Approaches in Surface Modifications of Dental Implants: A Literature Review. *Molecules* **2024**, *29*, 3061.
40. Maher, N.; Mahmood, A.; Fareed, M.A.; Kumar, N.; Rokaya, D.; Zafar, M.S. An Updated Review and Recent Advancements in Carbon-Based Bioactive Coatings for Dental Implant Applications. *J. Adv. Res.* **2024**.
41. Bonifacius, S.; Rikmasari, R.; Dirgantara, T.; Sukotjo, C.; Sulaiman, M.Y. A Biomechanical Finite Element Analysis of All-on-Four Concept Using Short Implants in Maxilla. *J. Int. Dent. Med. Res.* **2024**, *17*.
42. Liang, L.; Wu, X.; Yan, Q.; Shi, B. Are Short Implants (≤ 8.5 Mm) Reliable in the Rehabilitation of Completely Edentulous Patients: A Systematic Review and Meta-Analysis. *J. Prosthet. Dent.* **2024**, *131*, 826–832.
43. Strauss, F.J.; Gil, A.; Smirani, R.; Rodriguez, A.; Jung, R.; Thoma, D. The Use of Digital Technologies in Peri-implant Soft Tissue Augmentation–A Narrative Review on Planning, Measurements, Monitoring and Aesthetics. *Clin. Oral Implants Res.* **2024**.

44. Fuglsig, J.M. de C. e S.; Reis, I.N.R. dos; Yeung, A.W.K.; Bornstein, M.M.; Spin-Neto, R. The Current Role and Future Potential of Digital Diagnostic Imaging in Implant Dentistry: A Scoping Review. *Clin. Oral Implants Res.* **2024**, *35*, 793–809.
45. Truong, T.-D.-N.; Pradhan, A.M.S.; Nguyen, T.-T.; Tran, M.-H.; Nguyen, C.-K.; Ho, D.-D.; Huynh, T.-C. Bone-Implant Osseointegration Monitoring Using Electro-Mechanical Impedance Technique and Convolutional Neural Network: A Numerical Study. *J. Nondestruct. Eval.* **2024**, *43*, 10.
46. Robau-Porrua, A.; González, J.E.; Rodríguez-Guerra, J.; González-Mederos, P.; Navarro, P.; de la Rosa, J.E.; Carbonell-González, M.; Araneda-Hernández, E.; Torres, Y. Biomechanical Behavior of a New Design of Dental Implant: Influence of the Porosity and Location in the Maxilla. *J. Mater. Res. Technol.* **2024**, *29*, 3255–3267, doi:https://doi.org/10.1016/j.jmrt.2024.02.091.
47. Liu, L.; Ma, S.; Zhang, Y.; Zhu, S.; Wu, S.; Liu, G.; Yang, G. Parametric Design of Porous Structure and Optimal Porosity Gradient Distribution Based on Root-Shaped Implants. *Materials (Basel).* **2024**, *17*, 1137.
48. Alemayehu, D.B.; Huang, S.-J.; Koricho, E.G. Experimental and FEM Analysis of Three Carbon Steel Characterization under Quasi-Static Strain Rate for Bumper Beam Application. In Proceedings of the MATEC Web of Conferences; 2017; Vol. 123.
49. Alemayehu, Dawit Bogale;Masahiro, T. Enhanced Energy Absorption with Bioinspired Composite Triply Periodic Minimal Surface Gyroid Lattices Fabricated via Fused Filament Fabrication (FFF). *J. Manuf. Mater. Process.* **2024**, *8*, 86.
50. Alemayehu, D.B.; Jeng, Y.R. Three-Dimensional Finite Element Investigation into Effects of Implant Thread Design and Loading Rate on Stress Distribution in Dental Implants and Anisotropic Bone. *Materials (Basel).* **2021**, *14*, doi:10.3390/ma14226974.
51. Alemayehu, D.B.; Todoh, M.; Huang, S.J. Advancing 3D Dental Implant Finite Element Analysis: Incorporating Biomimetic Trabecular Bone with Varied Pore Sizes in Voronoi Lattices. *J. Funct. Biomater.* **2024**, *15*, doi:10.3390/jfb15040094.
52. Alemayehu, D.B. Design and Development of Shell and Tube Heat Exchanger for Harar Brewery Company Pasteurizer Application (Mechanical and Thermal Design). *Am. J. Eng. Res.* **2013**, *2*, 99–109.
53. Alshoaibi, A.M.; Fageehi, Y.A. Simulation of Quasi-Static Crack Propagation by Adaptive Finite Element Method. *Metals (Basel).* **2021**, *11*, 98.
54. Hisam, M.J.; Lim, J.Y.; Kurniawan, D.; Nor, F.M. Stress Distribution Due to Loading on Premolar Teeth Implant : A Three Dimensional Finite Element Analysis. *Procedia Manuf.* **2015**, *2*, 218–223, doi:10.1016/j.promfg.2015.07.038.
55. Williams, J.L. Anisotropic Elasticity of Cortical and Cancellous Bone in the Posterior Mandible Increases Peri-Implant Stress and Strain under Oblique Loading. **1995**, 648–657.
56. Chen, W.; Zhang, C.; Peng, S.; Lin, Y.; Ye, Z. Hydrogels in Dental Medicine. *Adv. Ther.* **2024**, *7*, 2300128.
57. Dechow, P.C.; Nail, G.A. Elastic Properties of Human Supraorbital and Mandibular Bone. **1993**, *306*, 291–306.
58. Liu, X.; Pang, F.; Li, Y.; Jia, H.; Cui, X.; Yue, Y.; Yang, X.; Yang, Q. Effects of Different Positions and Angles of Implants in Maxillary Edentulous Jaw on Surrounding Bone Stress under Dynamic Loading: A Three-Dimensional Finite Element Analysis. *Comput. Math. Methods Med.* **2019**, *2019*, doi:10.1155/2019/8074096.
59. Salavati, H.; Pullens, P.; Ceelen, W.; Debbaut, C. The Effect of a Necrotic Core on the Interstitial Fluid Pressure in Solid Tumors. In Proceedings of the 17th International Symposium on Computer Methods in Biomechanics and Biomedical Engineering and 5th Conference on Imaging and Visualization; 2021.
60. DIZAYEE, W.A.N.M.; IKRAM, F.S.; AL-AWWAL, D.B.J. COMPARISON BETWEEN CONVENTIONAL AND DIGITAL OCCLUSAL ANALYSIS.
61. Kurniawan, D.; Nor, F.M.; Lee, H.Y.; Finite, J.Y.L. Finite Element Analysis of Bone – Implant Biomechanics : Refinement through Featuring Various Osseointegration Conditions. *Int. J. Oral Maxillofac. Surg.* **2012**, *41*, 1090–1096, doi:10.1016/j.ijom.2011.12.026.
62. Am, O.M.; Jl, W.; Jo, K.; Anisotropic, S.P.; Williams, J.L.; Katz, J.O.; Spencer, P. Anisotropic Elastic Properties of Cancellous Bone from a Human Edentulous Mandible. **2000**, 415–421.
63. Lee, C.C.; Lin, S.C.; Kang, M.J.; Wu, S.W.; Fu, P.Y. Effects of Implant Threads on the Contact Area and Stress Distribution of Marginal Bone. *J. Dent. Sci.* **2010**, *5*, 156–165, doi:10.1016/S1991-7902(10)60023-2.